HHS Public Access

Author manuscript

Neurosci Lett. Author manuscript; available in PMC 2022 August 24.

Published in final edited form as:

Neurosci Lett. 2021 August 24; 760: 135974. doi:10.1016/j.neulet.2021.135974.

Subcellular localization of neuronal nuclei (NeuN) antigen in size and calcitonin gene-related peptide (CGRP) populations of dorsal root ganglion (DRG) neurons during acute peripheral inflammation

Michael B. Anderson, **Subhas Das**, **Kenneth E. Miller**

Michael Anderson, Oklahoma State University Center for Health Sciences, Anatomy & Cell Biology (E-453/461), 1111 W 17th St, Tulsa Oklahoma 74135

Abstract

Pseudo-unipolar cell bodies of somatosensory primary neurons are located in the dorsal root ganglia (DRG). The somatic and peripheral domains of DRG neurons are often studied in sensory pain research to understand molecular mechanisms involved in the activation of pain and maintenance of inflammation. Adjuvant-induced arthritis (AIA) is an inflammatory model that elicits a robust and rapid onset immune response with a maximal swelling period of 24–48 hours and persisting for several weeks. The AIA model in the hind paw of the rat elicits a potent inflammatory response of the dermis and epidermis, leading to protein expression changes for sensitization of many DRG neurons; however, it is unknown if the AIA model in the hind paw of the rat induces DRG neuronal injury, necrosis, or apoptosis at the somatic level. Neuronal nuclei (NeuN) antigen is a biomarker for post-mitotic neurons, neuronal identification, protein alterations, injury, and loss. Calcitonin gene-related peptide (CGRP) is expressed in C and Aδ DRG neurons, a subset of DRG neurons known to play a role in peripheral sensitization. The focus of the is research was to evaluate the expression pattern of NeuN immunoreactivity, in size (soma) and CGRP subpopulations of DRG neurons in naïve and inflamed groups. Confirmed by both immunofluorescence and immunoprecipitation, DRG neuronal expression of NeuN was localized to nuclear and cytoplasmic subcellular compartments. NeuN increased within the nucleus of small CGRP positive DRG neurons during inflammation, indicating a potential role for NeuN in a subset of nociceptive neurons.

Corresponding/First Author: Michael B. Anderson (michael.b.anderson@okstate.edu).

CRediT Author Statement

Michael B. Anderson was responsible for conceptualization, investigation, methodology, formal analysis, writing - original draft, writing - review & editing, and project administration. Dr. Kenneth E. Miller was responsible for conceptualization, methodology, resources, formal analysis, writing – review& editing, supervision, and funding acquisition. Dr. Subhas Das was responsible for methodology and formal analysis.

Declarations of Interest: Declarations of interest: none

Compliance with Ethical Statements: We know of no conflicts of interest associated with this publication, and there has been no significant financial support for this work that could have influenced its outcome. As Corresponding Author, I confirm that the manuscript has been read and approved for submission by all the named authors.

Keywords

neuronal nuclear (NeuN) antigen; calcitonin gene-related peptide (CGRP); primary afferent neurons; neuronal injury

Introduction

Primary sensory neurons of the somatosensory pathway project axons from the dorsal root (or spinal) ganglia (DRG) over great distances and terminate in peripheral tissue as multiple branched afferent nerve terminals. The complexity of pseudo-unipolar DRG neurons include four main functional domains: the peripheral terminal (environmental sensory activation), the DRG soma (gene and protein response), information conveyance (axon action potential), and the relay of information to the central nervous system (synaptic transmission). Altered action potential firing patterns and retrograde transport of neurotrophins during a severe inflammatory event can lead to short- and long-term adaptations of DRG neurons [8, 10]. Inflammation caused by disease and injury can result in a malfunction of this complex cellular processing, resulting in a maladaptation of neuronal plasticity and life-altering pain disorders. The cell bodies of primary sensory neurons often are studied to understand adaptive and maladaptive alterations during immune-regulated pain [15]. A common model for inducing peripheral inflammation is intradermal injection of complete Freund's adjuvant (CFA), peak swelling at 24–48 hours and persisting for several weeks [15]. The AIA model in the hind paw of the rat induces peripheral inflammation with increased mechanical sensitivity and a peak inflammation of 48-hours [17].

We and others have shown that DRG neuronal cell bodies upregulate the production of pro-sensitization proteins in the course of the CFA model [15, 16, 29]. During CFA-induced inflammation in the rat hind paw, dermal axons and intra-epidermal nerve fibers (IENFs) from the DRG are located within the inflammatory edema; however, it is unknown if the DRG neuronal cell body becomes injured, necrotized, or apoptotic during the peak swelling event.

To evaluate neuronal plasticity, injury, or loss, we chose Neuronal Nuclei (NeuN), a neuronal biomarker involved in transcriptional regulation. The NeuN antigen is a 106 amino-acid epitope mapped to the N-terminal of forkhead box (FOX)-3 protein [20] and is expressed in the nuclei of post-mitotic neurons [27]. The function of NeuN/FOX-3 is a post-mitotic splicing regulator using cell-specific alternative splicing in the nuclei of most neurons [9, 20]. While the NeuN antigen was originally reported exclusive to neuronal nuclei, it has since been determined to be in neuronal-cytoplasm, both, or completely absent [11, 23, 35]. NeuN/FOX-3 expression is variable, including increasing, decreasing, or not changing, in different experimental models. In rat hippocampal neurons and mouse motor neurons, NeuN/FOX-3 expression can be stimulated to increase [2, 23, 30]. A loss of NeuN antigenicity occurs in certain neuronal injury models, while neurons appear to be functioning, with a reappearance of NeuN/FOX-3 immunoreactivity (IR) at later timepoints [26, 34]. Alternatively, models causing neuronal injury or neuronal death often show a decrease in NeuN/FOX-3 expression [4, 26, 31, 37].

CGRP is a potent vasodilator, expressed in C and Aδ neurons, and functions in the transmission of nociceptive signaling and inflammatory wound healing [18]. While CGRP positive (+) and CGRP negative (−) DRG neurons both play a role in nociception and peripheral sensitization, they are functionally different [3]. Evaluation of CGRP in DRG neurons was performed in the present study to examine subsets of DRG neurons involved in the acute peripheral sensitization at a peak AIA time point. AIA was induced in the rat hind paw and NeuN/FOX-3 IR in the nucleus and cytoplasm of L4 DRG neurons was evaluated in CGRP (+) and CGRP (−) subpopulations. Nuclear and cytoplasmic subfractionation of DRG neurons followed by NeuN/FOX-3 immunoblotting was used to verify immunohistochemical data. To further investigate the integrity of DRG neuronal nuclei in the AIA model, 4',6-diamidino-2-phenylindole (DAPI) fluorescence was measured for area, perimeter and mean grey intensity (MGI). We hypothesized that all DRG neurons express NeuN/FOX-3 while retaining neuronal viability at the peak swelling point of the AIA model. We expected an increase in NeuN/FOX-3 expression due to an increased demand of RNA splicing during inflammatory conditions. However, if DRG neuronal injury or loss occurs, NeuN/FOX-3 was expected to decrease, indicating a reduction of transcription in some DRG neurons.

Methods

Animals

Male and female Sprague Dawley rats (Charles River; n=21 150–250 grams; 8 weeks of age) were bred, maintained on-site, and used in IHC and Western blot experiments. All rats were given food and water *ad libitum* and housed with a 12-hour on/off light cycle. All methods and techniques utilized in these experiments were conducted in accordance of the National Institute of Health (NIH, https://www.ncbi.nlm.nih.gov/books/NBK43327/), the International Association for the Study of Pain (IASP, https://www.ncbi.nlm.nih.gov/pubmed/6877845), and approved by the Oklahoma State University Center for Health Sciences Institutional Animal Care and Use Committee (2016–03). All efforts were made to care for and minimize the total number of rats used in these experiments to reduce potential suffering.

48-hour Adjuvant-Induced Arthritis Model

Complete Freund's adjuvant (CFA) was emulsified in a 1:1 ratio with phosphate buffered saline (PBS) and injected into the right hind paw of experimental animals to establish unilateral adjuvant-induced arthritis. For IHC (n=9) and Western blot analysis (n=12), all rats (n 21) were housed for 48-hours with food and water provided *ad libitum.* The AIA group were anesthetized with isoflurane (1.5 liters'/minute oxygen, 2% isoflurane) and injected with 150 μl emulsified CFA in the center of the right hind paw with a 26-gauge needle, and allowed to recover. The metatarsal region of the right hind paw of all animals was measured with a dial caliper shortly before transcardial perfusion [15].

Immunohistochemistry

After 48 hours, rats (n=9) were deeply anesthetized with Avertin, a tribromoethanol anesthesia, diluted at 2.5% *(v/v)* in PBS (pH: 7.3) and administered intraperitoneally (IP)

[15, 36]. To determine level of anesthesia, a three-point flinch test was performed on the eye, tail, and hind paw. Once rats were determined unresponsive, 1.0 ml xylazine (100mg/ml) was delivered IP and approximately 1 minute later rats were transcardially perfused with 100 ml calcium-free tyrodes (pH:7,3), followed by fixative. Transcardial perfusions were performed with a peristaltic pump at a rate of 37 ml/minute and a total volume of 425 ml of fixative, per rat. Rats were perfused with a modified Zamboni's fixative: 0.75% *(w/v)* picric acid, 0.2% *(w/v)* paraformaldehyde (PFA), phosphate buffered saline (PBS, pH: 7.3) [15]. This low aldehyde fixative has been shown to provide optimal labelling in DRG neurons [15]. The right ipsilateral lumbar 4 DRG were collected, and post-fixed for 3 hours at 4°C and transferred into PBS with 10% *(w/v,* pH 7.3) sucrose, overnight [5, 22]. DRGs were placed into a single mold with M1 embedding matrix and frozen with liquid nitrogen. Frozen DRG sections (12 μm) were cut on a Leica cryostat and thaw-mounted on gelatin-coated glass slides. All slides were dried for 60 minutes on a slide warmer (37°C) before antibody incubations and PBS washing steps. Primary antibody were diluted in PBS with 0.5% *(w/v)* bovine serum albumin (BSA), 0.5% *(w/v)* polyvinylpyrollidone (PVP), and 0.3% *(v/v)* Triton-X100, pH: 7.3. Chicken polyclonal NeuN antisera (Millipore, ABN91, RRID:AB_11205760) was diluted to 0.5 μg/ml (1:1000). Mouse monoclonal antibody for CGRP was diluted to 0.1 μg/ml (1:2000) (Santa Cruz, 57053, RRID:AB_2259462) [13]. Nuclear staining was achieved by using DAPI at a concentration of 300 nM (ThermoFisherScientific D3571, RRID:AB_2307445). Antibodies raised against NeuN and CGRP were combined for multiplex labeling in PBS-BSA-PVP-Triton-X (pH, 7.3). Slide containers were sealed with parafilm to prevent evaporation and placed on a rocker at 4°C for 96 hours. All slides were were washed three times in PBS for 10 minutes each at room temperature to remove unbound antisera. Tissue was incubated in secondary antisera with donkey anti-chicken 488 (JacksonImmunoResearchLabs, 703–545-155, RRID:AB_2340375) and donkey anti-mouse Alexa Fluor 647 (ThermoFisherScientific, A-31571, RRID:AB_162542). Secondary antibodies w ere diluted to 1 μg/ml (1:1000) in PBS with 0.3% (*v/v*) Triton-X100, combined for multiplex labeling, and incubated on a rocker for one hour at room temperature. During secondary incubation, and subsequent incubation steps, all slide containers were covered with aluminum foil to prevent fluorophore bleaching from ambient light. Slides were washed three times in PBS, incubated in 300nM DAPI for 15 minutes, and washed three times in PBS before cover-slipping in Prolong Gold anti-fade mounting media.

Imaging

Images were collected on a BX51TRF Olympus epifluorescence microscope with a SPOT-RT470 camera at a pixel resolution of 1024×1024, and saved in *.tiff format. Camera exposures used for experimental evaluation were determined before image acquisition for data collection and unchanged throughout the imaging process. One image per channel was taken, per field of view (FOV), with an Olympus UPlanFL 20×/0.50, ∞0.17 objective for NeuN (exposure: 250 milliseconds (ms), gain: 2), CGRP (exposure: 2.5 seconds, gain: 2), and DAPI (exposure: 400 ms, gain: 2). Sampling of the FOVs were randomly selected for high density of DRG neurons and collected from different slides and sections. As in our previous studies, a threshold for differentiating CGRP (+) from CGRP (−) DRG neurons was

determined by the frequency distribution and smooth spline fitting of CGRP IR in all naive DRG neurons [15, 16, 36]

Experimental Design: Manual Tracing

All images were manually hand traced in ImageJ version 1.48v [32], using a Wacom Cintiq 21UX monitor. DRG neuronal size is related to action potential conduction velocity and is loosely correlated with function; accordingly, we measured and categorized all neurons as small (<400 μm^2), medium (400 – 800 μm^2), or large (>800 μm^2) [12]. The ascending order of CGRP IR was evaluated by frequency distribution and then smooth spline fitting, with 4 knots, to determine the threshold for CGRP (8-bit range of CGRP: 39–255) for classifying DRG neurons as CGRP (+) or CGRP (−) [33].

Subcellular Fractionation

Right L4 and L5 DRGs were dissected from each rat (n=8) [22]. DRGs were immediately minced and placed in 1.5 micro-centrifuge tubes with 200 µl STM buffer and 2 µl protease inhibitor, then processed using a previously reported technique [7].

Immunoblot analysis

Subfractionated samples were measured with a BCA assay kit to standardize protein concentration. All samples were processed for electrophoresis by adding 10 µl loading dye (0.25 mmol/L Tris, 50% glycerol, 2% sodium dodecyl sulfate (SDS), 0.01% bromophenol blue, and 50 µl/ml β-mercaptoethanol, pH: 6.8) to 40 µg protein, per sample, and boiled at 100°C, for 10 minutes. Purified protein was loaded at a concentration of 40 µg total protein per lane and processed with Bio-Rad 7.5% TGX acrylamide kit (Bio-Rad, 1610171). Electrophoresis was performed in running buffer (191.8 mmol/L glycine, 24.8 mmol/L Tris, and 3.5 mmol/L SDS) at 100 V for 15 minutes and 150 V for 40 minutes. Proteins were transferred onto nitrocellulose membranes, in transfer buffer (191.8 mmol/L glycine, 24.8 mmol/L Tris, and 20% methanol), and incubated in PBS-tween with 5% BSA. PBS with 0.3% tween was used in all steps. Chicken polyclonal NeuN antiser a was diluted 0.5 µg/ml (1:1000). Mouse anti-lamin B (ThermoFisherScientific, 33–2000, RRID:AB_2533106) normalized nuclear signals and was diluted 2.5 µg/ml (1:200) (Invitrogen, 33–2000, RRID:AB_2533106). Rabbit anti-GAPDH (Cell Signaling Technology, 2118S, RRID:AB_561053) normalized cytoplasmic signals and was diluted 0.014 µg/ml (1:3000).Primary antibodies were visualized by donkey anti-chicken 488 (JacksonImmunoResearchLabs, 703–545-155, RRID:AB_2340375) and donkey anti-mouse Alexa Fluor 647 (ThermoFisherScientific, A-31571, RRID:AB_162542) secondary antibodies, diluted to 1 µg/ml (1:1000). Immunoblots were imaged on a Typhoon Scanner 9410.and all channels were visualized at 500 V. Data for NeuN/FOX-3 protein concentration were normalized by CTR lanes and analyzed in Graphpad Prism 8.

Statistical Analysis

Power analysis (α=0.05, power=0.80, mean 1=100, mean 2=120) indicated a sample size of n=4 for each of our groups (https://clincalc.com/stats/samplesize.aspx), therefore n=4 for naïve and n=4 for AIA, per IHC and WB techniques. Evaluation of NeuN/FOX-3

IR, hind paw edema, and Western blots were processed in Graphpad Prism 8. Hind paw edema was quantified by comparing the metatarsal means from naive CTR (n=4) and AIA (n=4) conditions. The grand mean of NeuN/FOX-3 IR between naive and AIA groups were compared with the Mann-Whitney test. Significance was determined when the p-value was less than 0.05. Normality of the grand mean (CTR, n=4; AIA, n=4), f ~ one-way ANOVA analysis, of NeuN/FOX-3 IR was analyzed by the Shapiro-Wilk test. Multiple comparisons were statistically evaluated by parametric one-way ANOVA with Tukey post-hoc analysis. Significance was determined when the p-value was less than 0.05. Cytoplasmic and nuclear lanes of Western blots were normalized by GAPDH and lamin B lanes, respectively, and plotted in Graphpad Prism 8. Data from the cytoplasm o naive rat three was removed due to a faint, although visibly present, GAPDH band. Western blot data were analyzed for normality by the Shapirio-Wilk test and statistically evaluated by parametric Student's t-test. Significance was determined when the p-value was less than 0.05.

Results

Hind Paw Edema

There was a significant difference (p=0.0286) in metatarsal thickness between naive (IHC, n=4, mean=3.45 mm, standard deviation (SD)=0.5492; WB, n=4, mean=3.363 mm, SD=0.3301) and AIA (IHC, n=4, mean=8.11 mm, SD=0.2839; WB, n=4, mean=7.5 mm, SD=0.2839) rats for IHC and for subcellular fractionation/WB experiments, respectively. The increase of hind paw thickness for rats in IHC experiments was 2.35-fold and 2.23-fold in WB experiments.

Imaging

All images were collected from 3–5 slides, 3–5 sections per L4 DRG, yielding 3–5 total FOVs per rat. There were at least 135 neurons evaluated per group, except for rat 7 from the AIA group (Table 1). Many FOVs from Rat 7 contained mostly axons, resulting in fewer evaluated sections and measured neurons than other groups (Table 1). Evaluation of CGRP IR in naïve rats by frequency distribution and smooth spline fitting, with 4 knots, indicated that an 8-bit mean grey intensity value of 39 as a reliable threshold, differentiating CGRP (+) from CGRP (−) DRG neurons (Fig. 1).

NeuN/FOX-3 expression in DRG neurons

In both naïve and AIA conditions, NeuN IR MGI was relatively consistent in total and CGRP sub-populations, except for nuclei of CGRP (+) neurons (Table 1, 2; Fig 2). In CGRP (+) neurons, NeuN IR MGI was greater in the cytoplasm and nuclei of medium-and large-sized neurons than small neurons (Table 1; Fig. 3). In AIA rats, NeuN IR MGI was larger in both the cytoplasm and nucleus of large CGRP (+) neurons than small CGRP (+) neurons (Table 1; Fig. 3). Furthermore, no statistical differences were found within CGRP (−) and CGRP (+) neurons, despite CFA-induced peripheral inflammation. (Table 2; Fig. 3). Nuclear NeuN IR increased significantly, from naïve to AIA conditions, by 27.3% in small CGRP (+) nuclei, whereas there was no increase in the cytoplasm (Fig. 4). There was no significant difference in the average number of CGRP (+) neurons between naïve and AIA groups. Qualitatively, DRG neurons from the naïve group exhibited a larger range of IR

(from light to intensely labeled) of NeuN/FOX-3 IR within the same size populations than DRG neurons from the inflammatory group (intensely labeled) (Fig. 5, A, E). Furthermore, many neurons in the AIA group which were positive for CGRP were also intensely labeled for NeuN/FOX-3 IR (Fig. 5, D, H).

DAPI labeling in DRG Neuronal Nuclei

Previous reports haves shown that a reduction of nuclear area and nuclear perimeter, defined by DAPI, is observed in apoptotic cell nuclei [24]. To evaluate neuronal integrity, we measured DAPI labeled DRG neuronal nuclei between naïve and AIA experimental conditions for DRG neuronal nuclei for area, perimeter and MGI. There were no significant differences of DRG neuronal nuclear DAPI MGI, area, or perimeter between any groups.

Western Blots

Anti-NeuN labels Fox-3 gene products as a doublet, typically from 45–50 kDa, and often a second doublet at ~70 kDa. The first doublet (45–50 kDa) are the NeuN antigens described by Mullen *et al* and the second doublet at 70 kDa was identified by Kim *et al* as primarily synapsin I [20, 27]. Two NeuN/FOX-3 doublets were observed at 46/48~ kDa and 64–66 kDa (Fig. 6, A, C). The cytoplasmic control, GAPDH, was exclusively present in the cytoplasmic lanes at 40 kDa (Fig. 6, A). The nuclear control, lamin B, resulted in a specific band at 70 kDa in the nuclear lanes (Fig. 6, C). The relative expression of NeuN/FoX-3 protein in cytoplasmic and nuclear CTR and AIA lanes determined for normal distribution and statistically evaluated by parametric t-test, resulted in no significance, respectively ($p= 0.5521$, $p = 0.0752$, Fig. 6, B, D).

Discussion

The repeated activation of DRG nerve terminals during inflammation coerces DRG somatic upregulation of CGRP and several pro-inflammatory (~6), pro-nociceptive (~16), and pro-apoptotic (~8) factors [18, 19, 25], a genomic symphony of mRNA transcription and protein translation. NeuN/FOX-3 is a splicing regulator, a protein involved in transcription, and thus we expected it to increase as neurons respond to peripheral inflammation. NeuN/FOX-3 expression is elevated in some central neurons, such as rat hippocampal neurons when stimulated with IP3 and sigma receptor antagonists and telomerase increasing compounds [6, 38]. NeuN/FOX-3 levels also rise in the cytoplasm of motor neurons in G93A SOD1 mice as the animals age [28]. In the current study, an increase of NeuN/FOX-3 IR occurred in DRG neuronal nuclei of small diameter neurons, a size population of DRG neurons responsive to inflammation. This is an indication that a subset of nociceptive neurons is responding to peripheral inflammation through a NeuN/FOX-3 mechanism. NeuN/FOX-3 regulates pre-mRNA splicing by interacting with protein associated splicing factor (PASF) and binding to the UGCAUG RNA element [21]. Future studies should involve evaluation of the specific RNAs regulated by NeuN/FOX-3 and PASF in response to peripheral inflammation.

We also considered that AIA might decrease NeuN/FOX-3 in some DRG neurons. The AIA model produces a disruptive blister in the epidermis and dermis, but it is unknown

whether potential peripheral loss of axon and terminal DRG neuronal domains in the blister region results in a loss of neuronal integrity or apoptosis. Models causing neuronal injury or neuronal death often show a decrease in NeuN/FOX-3 expression, such as: peripheral (facial) nerve crush rebounding at 28 days [26, 34], soman poisoning by 24-hours [4], blast pressure [31], irradiation [37], and different ischemic models [6, 28, 34]. In the central fluid percussion injury model in rats, however, NeuN/FOX-3 did not change at any timepoint in the lateral neocortex [14]. A loss of NeuN immunoreactivity occurs in certain neuronal assault models, while neurons appear to be functioning, with a later reappearance of NeuN/FOX-3 IR after 2–3 weeks [26, 34]. Based on these studies and considering its post-mitotic functionality, NeuN/FOX-3 has become known as a reference for neuronal viability and possibly a surrogate marker for irreversible nerve injury, but not as a strict marker for apoptosis [1, 9, 34]. In the current study, there was no decrease in observed NeuN/FOX-3 IR with either immunohistochemistry or subcellular fractionation and western blotting. With DAPI fluorescence, there were no signs of chromatin condensation or DNA fragmentation. These data, therefore, indicate there are no signs of DRG neuronal injury at the 48-hour timepoint of the AIA model.

In summary, CFA or the inflammation skin blister do not appear to cause a severe injury of DRG neurons at 48-hours of AIA. Assessing NeuN/FOX-3 or other injury related proteins at additional AIA time points or peripheral injury models may shed light on the reach on of DRG neurons to peripheral trauma. NeuN/FOX-3, however, did increase in small CGRP (+) neurons indicating a unique role for this transcription regulator in a subset of nociceptive neurons. Evaluating the mechanism of action for NeuN/FOX-3 during acute inflammation may provide a new therapeutic target for controlling pain.

Supplementary Material

Refer to Web version on PubMed Central for supplementary material.

Acknowledgements

This research was supported by National Institutes of Health, grant AR047410, awarded to Kenneth E. Miller, PhD.

Funding Statement:

This research was supported by National Institutes of Health grant AR047410, awarded to Kenneth E. Miller, PhD. The funding source (NIH) was not involved in design of the study, collection of data, analysis, and interpretation of the data.

All applicable international, national, and/or institutional guidelines for the care and use of animals were followed.

References

[1]. Alekseeva OS, Gusel'nikova VV, Beznin GV, Korzhevskii DE, Prospects of the nuclear protein NeuN application as an index of functional state of the vertebrate nerve cellsZh Evol Biokhim Fiziol51 (2015) 313–323. [PubMed: 26856070]

[2]. Baruch-Eliyahu N, Rud V, Braiman A, Priel E, Telomerase increasing compound protects hippocampal neurons from amyloid beta toxicity by enhancing the expression of neurotrophins and plasticity related genes, Sci Rep9 (2019) 18118. [PubMed: 31792359]

[3]. Breese NM, George AC, Pauers LE, Stucky CL, Peripheral inflammation selectively increases TRPV1 function in IB4-positive sensory neurons from adult mouse, Pain115 (2005) 37–49. [PubMed: 15836968]

[4]. Collombet JM, Masqueliez C, Four E, Burckhart MF, Bernabe DBabichon D, Lallement G, Early reduction of NeuN antigenicity induced by soman poisoning in mice can be used to predict delayed neuronal degeneration in the hippocampus, Neurosci Lett398 (2006) 337–342. [PubMed: 16472911]

[5]. da Silva Serra I, Husson Z, Bartlett JD, Smith ES, Characterization of cutaneous and articular sensory neurons, Mol Pain12 (2016).

[6]. Davoli MA, Fourtounis J, Tam J, Xanthoudakis S, Nicholson D, Robertson GS, Ng GY, Xu D, Immunohistochemical and biochemical assessment of caspase-3 activation and DNA fragmentation following transient focal ischemia in the rat, Neuroscience115 (2002) 125–136. [PubMed: 12401327]

[7]. Dimauro I, Pearson T, Caporossi D, Jackson MJ, A simple protocol for the subcellular fractionation of skeletal muscle cells and tissue, BMC Res Notes5 (2012) 513. [PubMed: 22994964]

[8]. Djouhri L, Koutsikou S, Fan g S XMcMullan S.N. Lawson, Spontaneous pain, both neuropathic and inflammatory, is related to frequency of spontaneous firing in intact C-fiber nociceptors, J Neurosci26 (2006) 1281–1292. [PubMed: 16436616]

[9]. Duan W, Zhang YP, Hou Z, Huang C, Zhu H, Zhang CQ, Yin Q, Novel Insights into NeuN: from Ne Tonal Marker to Splicing Regulator, Mol Neurobiol53 (2016) 1637–1647. [PubMed: 25680637]

[10]. Fang X, Djouhri L, McMullan S, Berry C, Okuse K, Waxman SG, Lawson SN, trkA is expressed in nociceptive neurons and influences electrophysiological properties via Nav1.8 expression in rapidly conducting nociceptors, J Neurosci25 (2005) 4868–4878. [PubMed: 15888662]

[11]. Gusel'nikova VV, Korzhevskiy DE, NeuN As a Neuronal Nuclear Antigen and Neuron Differentiation Marker, Acta Naturae7 (2015) 42–47. [PubMed: 26085943]

[12]. Harper A.A.l., S. N., Conduction velocity is related to morphological cell type in rat dorsal root ganglion neurones., Journal of Physiology (1985) 31–46.

[13]. He W, Long T, Pan Q, Zhang S, Zhang Y, Zhang D, Qin G, Chen L, Zhou J, Microglial NLRP3 inflammasome activation mediates IL-1beta release and contributes to central sensitization in a recurrent nitroglycerin-induced migraine model, J Neuroinflammation16 (2019) 78. [PubMed: 30971286]

[14]. Hernandez ML, Chatlos T, Gorse KM, Lafrenaye AD, Neuronal Membrane Disruption Occurs Late Following Diffuse Brain Trauma in Rats and Involves a Subpopulation of NeuN Negative Cortical Neurons, Front Neurol10 (2019) 1238. [PubMed: 31824411]

[15]. Hoffman EM, Schechter R, Miller KE, Fixative composition alters distributions of immunoreactivity for glutaminase and two markers of nociceptive neurons, Nav1.8 and TRPV1, in the rat dorsal root ganglion, J Histochem Cytochem58 (2010) 329–344. [PubMed: 20026672]

[16]. Hoffman EM, Zhang Z, Anderson MB, Schechter R, Miller KE, Potential mechanisms for hypoalgesia induced by anti-nerve growth factor immunoglobulin are identified using autoimmune nerve growth factor deprivation, Neuroscience193 (2011) 452–465. [PubMed: 21802499]

[17]. Hoffman EM, Zhang Z, Schechter R, Miller KE, Glutaminase Increases in Rat Dorsal Root Ganglion Neurons after Unilateral Adjuvant-Induced Hind Paw Inflammation, Biomolecules6 (2016) 10. [PubMed: 26771651]

[18]. Iyengar S, Ossipov MH, Johnson KW, The role of calcitonin gene-related peptide in peripheral and central pain mechanisms including migraine, Pain158 (2017) 543–559. [PubMed: 28301400]

[19]. Ji RR, Samad TA, Jin SX, Schmoll R, Woolf CJ, p38 MAPK activation by NGF in primary sensory neurons after inflammation increases TRPV1 levels and maintains heat hyperalgesia, Neuron36 (2002) 57–68. [PubMed: 12367506]

[20]. Kim KK, Adelstein RS, Kawamoto S, Identification of neuronal nuclei (NeuN) as Fox-3, a new member of the Fox-1 gene family of splicing factors, J Biol Chem284 (2009) 31052–31061. [PubMed: 19713214]

[21]. Kim KK, Kim YC, Adelstein RS, Kawamoto S, Fox-3 and PSF interact to activate neural cell-specific alternative splicing, Nucleic Acids Res39 (2011) 3064–3078. [PubMed: 21177649]

[22]. Lin YT, Ro LS, Wang HL, Chen JC, Up-regulation of dorsal root ganglia BDNF and trkB receptor in inflammatory pain: an in vivo and in vitro study, J Neuroinflammation8 (2011) 126. [PubMed: 21958434]

[23]. Ma X, Turnbull PC, Crapper EP, Wang H, Drannik A, Jiang F, Xia S, Turnbull J, Cytosolic localization of Fox proteins in motor neurons of G93A SOD1 mice, Histochem Cell Biol145 (2016) 545–559. [PubMed: 26724814]

[24]. Mandelkow R, Gumbel D, Ahrend H, Kaul A, Zimmermann U, Burchardt M, Stope MB, Detection and Quantification of Nuclear Morphology Changes in Apoptotic Cells by Fluorescence Microscopy and Subsequent Analysis of Visualized Fluorescent Signals, Anticancer Res37 (2017) 2239–2244. [PubMed: 28476788]

[25]. Martin SL, Reid AJ, Verkhratsky A, Magnaghi V, Faroni A, Gene expression changes in dorsal root ganglia following peripheral nerve injury: roles in inflammation, cell death and nociception, Neural Regen Res14 (2019) 939–947. [PubMed: 30761997]

[26]. McPhail LT, McBride CB, McGraw J, Steeves JD, Tetzlaff W, Axotomy abolishes NeuN expression in facial but not rubrospinal neurons, Exp Neurol185 (2004) 182–190. [PubMed: 14697329]

[27]. Mullen RJ, Buck CR, Smith AM, NeuN, a neuronal specific nuclear protein in vertebrates, Development116 (1992) 201–211. [PubMed: 1483388]

[28]. Portiansky EL, Barbeito CG, Gimeno EJ, Zuccolilli GO, Goya RG, Loss of NeuN immunoreactivity in rat spinal cord neurons during aging, Exp Neurol202 (2006) 519–521. [PubMed: 16935281]

[29]. Qu L, Caterina MJ, Enhanced excitability and suppression of A-type K(+) currents in joint sensory neurons in a murine model of antigen-induced arthritis, Sci Rep6 (2016) 28899. [PubMed: 27363579]

[30]. Reynolds AR, Saunders MA, Prendergast MA, Ethanol Stimulates Endoplasmic Reticulum Inositol Triphosphate and Sigma Receptors to Promote Withdrawal-Associated Loss of Neuron-Specific Nuclear Protein/Fox-3, Alcohol Clin Exp Res40 (2016) 1454–1461. [PubMed: 27177604]

[31]. Sajja VS, Ereifej ES, VandeVord PJ, Hippocampal vulnerability and subacute response following varied blast magnitudes, Neurosci Lett570 (2014) 33–37. [PubMed: 24726403]

[32]. Schneider CA, Rasband WS, Eliceiri KW, NIH Image to ImageJ: 25 years of image analysis, Nat Methods9 (2012) 671–675. [PubMed: 22930834]

[33]. Schou WS, Ashina S, Amin FM, Goadsby PJ, Ashina M, Calcitonin gene-related peptide and pain: a systematic review, J Headache Pain18 (2017) 34. [PubMed: 28303458]

[34]. Unal-Cevik I, Kilinc M, Gursoy-Ozdemir Y, Gurer G, Dalkara T, Loss of NeuN immunoreactivity afte cerebral ischemia does not indicate neuronal cell loss: a cautionary note, Brain Res1015 (2004) 169–174. [PubMed: 15223381]

[35]. Van Nassauw L, Wu M, De Jonge F, Adriaensen D, Timmermans JP, Cytoplasmic, but not nuclear, expression of the neuronal nuclei (NeuN) antibody is an exclusive feature of Dogiel type II neurons in the guinea-pig gastrointestinal tract, Histochem Cell Biol124 (2005) 369–377. [PubMed: 16049694]

[36]. Wang T, Miller KE, Characterization of glutamatergic neurons in the rat atrial intrinsic cardiac ganglia that project to the cardiac ventricular wall, Neuroscience329 (2016) 134–150. [PubMed: 27167082]

[37]. Wu KL, Li YQ, Tabassum A, Lu WY, Aubert I, Wong CS, Loss of neuronal protein expression in mouse hippocampus after irradiation, J Neuropathol Exp Neurol69 (2010) 272–280. [PubMed: 20142763]

[38]. Natalie Baruch-Eliyahu, Vladislav Rud, Alex Braiman, Esther PrielTelomerase increasing compound protects hippocampal neurons from amyloid beta toxicity by enhancing the expression of neurotrophins and plasticity related genesSci. Rep69 (2019) 10.1038/s41598-019-54741-7

Highlights

- Neuronal Nuclei (NeuN) protein is expressed in the nucleus and cytoplasm of DRG neurons
- Increased NeuN/FOX-3 expression in DRG neurons indicates a robust neuronal response at the peak swelling timepoint of CFA-induced acute inflammation
- No morphologic signs of nuclear shrinking, chromatin condensation, or DNA fragmentation were observed in DRG neurons of any inflammatory group
- These data suggest that there are no signs of DRG neuronal suffering or injury at the 48-hour timepoint of the AIA model in the hind paw of the rat

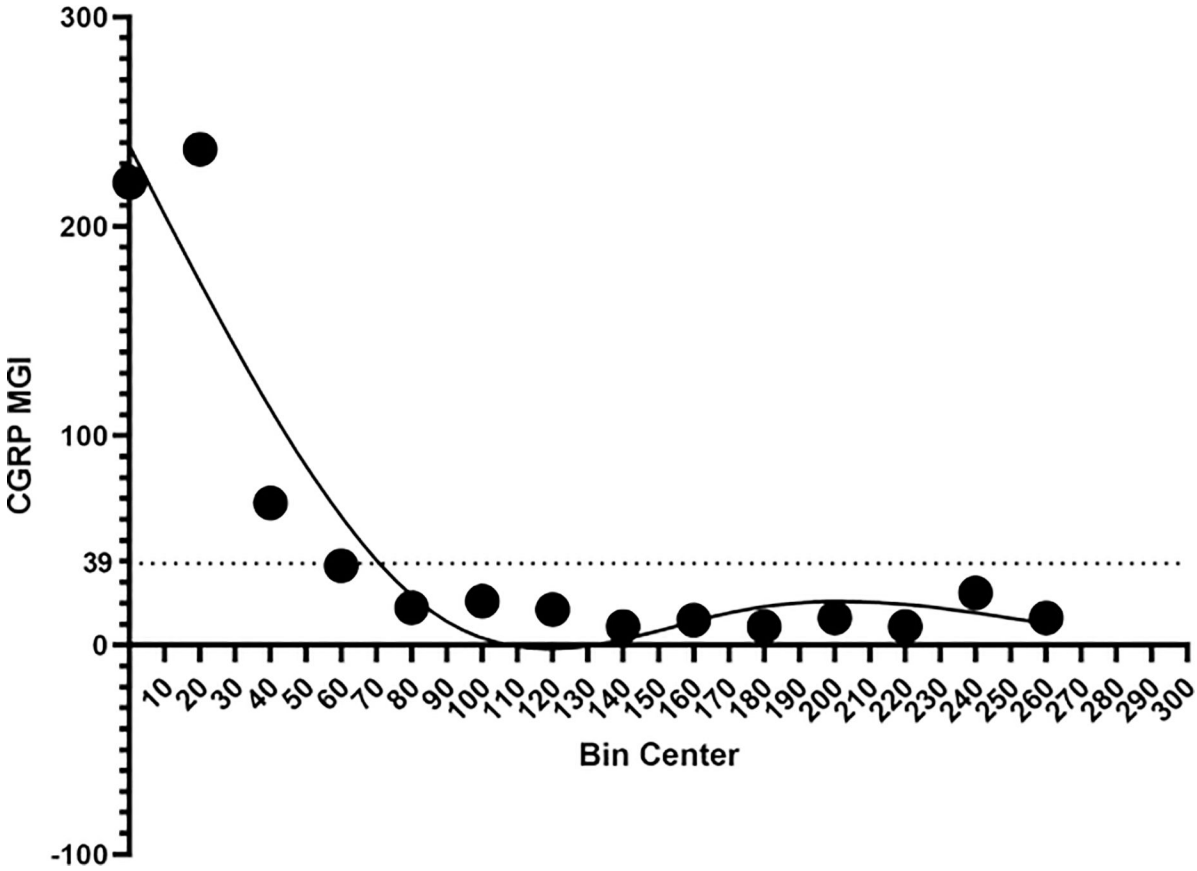

Figure 1:

Evaluation of CGRP IR in naïve rats by frequency distribution and smooth spline fitting, with 4 knots, indicated that an 8-bit mean grey intensity (0–255) value of 39 as a reliable threshold, differentiating CGRP (+) from CGRP (−) DRG neurons.

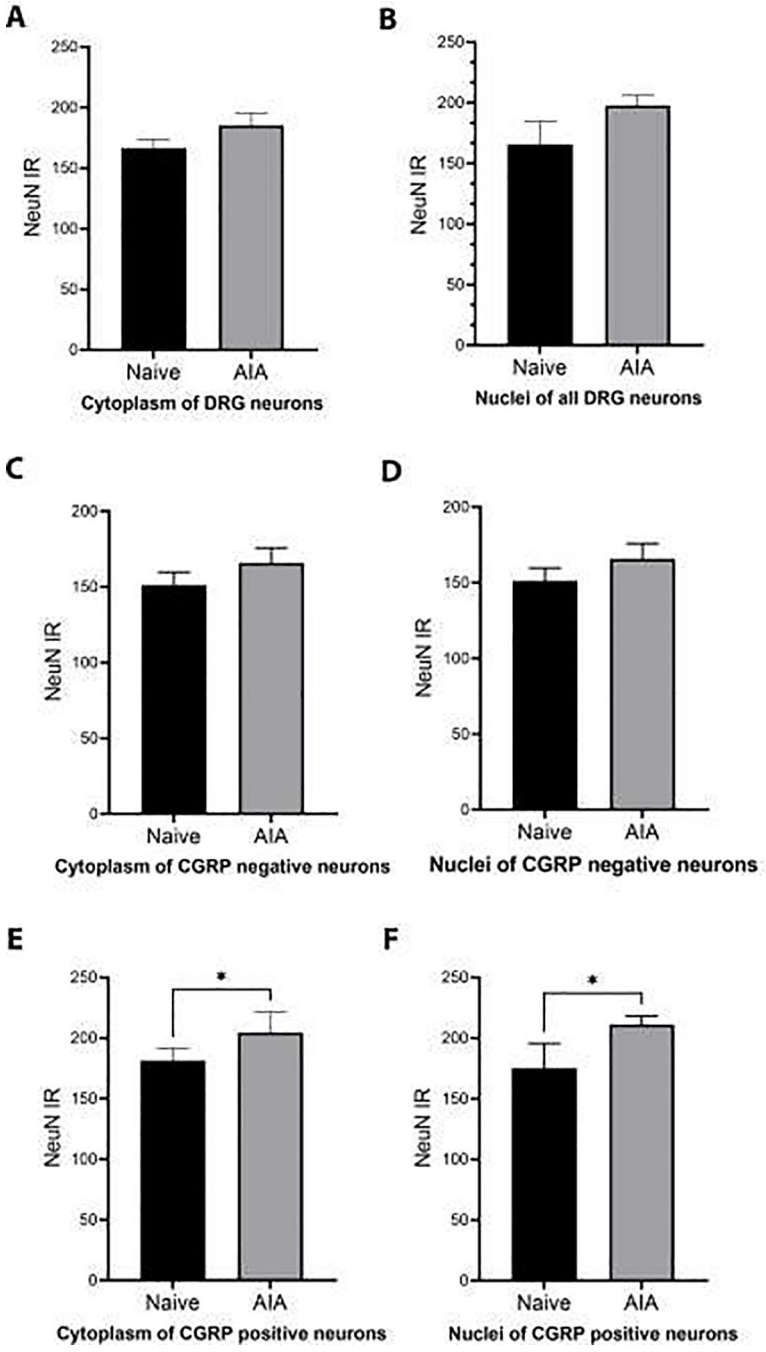

Figure 2: Naïve and AIA comparison of NeuN IR in DRG total DRG neurons, CGRP (−) neurons, and CGRP (+) neurons.

A, no significant differences found between naïve and AIA cytoplasm (p=0.0571, Δ=17.96) and nucleus (p=0.0571, Δ=39.47). B, no significant differences found between CGRP (−) cytoplasm (p=0.1143, Δ=14.44) and nucleus (p=0.1143, Δ=14.44). C, significant differences found between CGRP (+) cytoplasm (p=0.0286, Δ=17.35) and nucleus (0.0286, Δ=41.15).

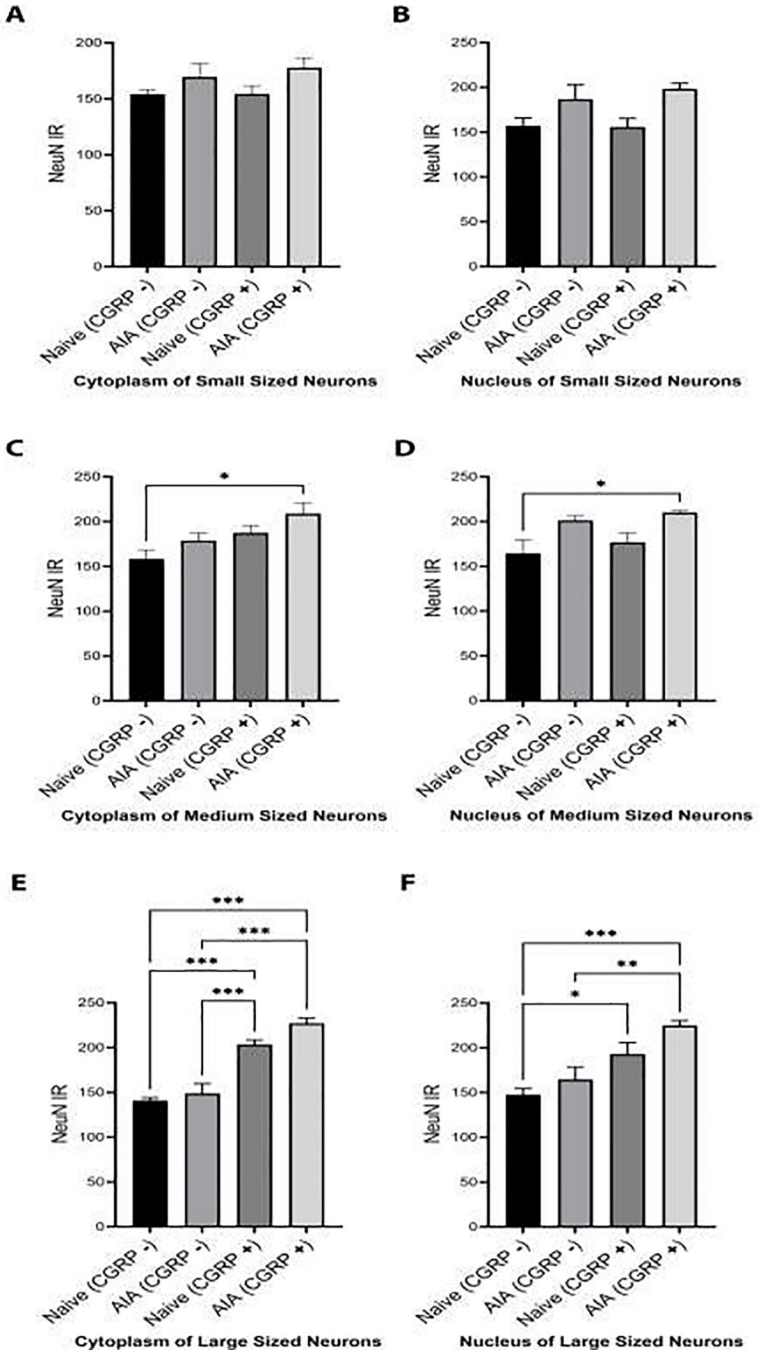

Figure 3: Evaluation of NeuN IR between condition (naïve/AIA) and CGRP (−) and CGRP (+) neurons.

A-B, no significant differences found in cytoplasm or nucleus of small neurons. **C-D**. Significant differences were found in the cytoplasm ($F(3, 12)=4.441$, $p=0.026$) and nucleus ($F(3, 12)=4.60$, $p=0.023$) of medium neurons-**F**, Significant differences found in cytoplasm ($F(3, 12)=36.09$, $p<.001$) and nucleus ($F(3, 12)=11.03$, $p<.001$) of large neurons.

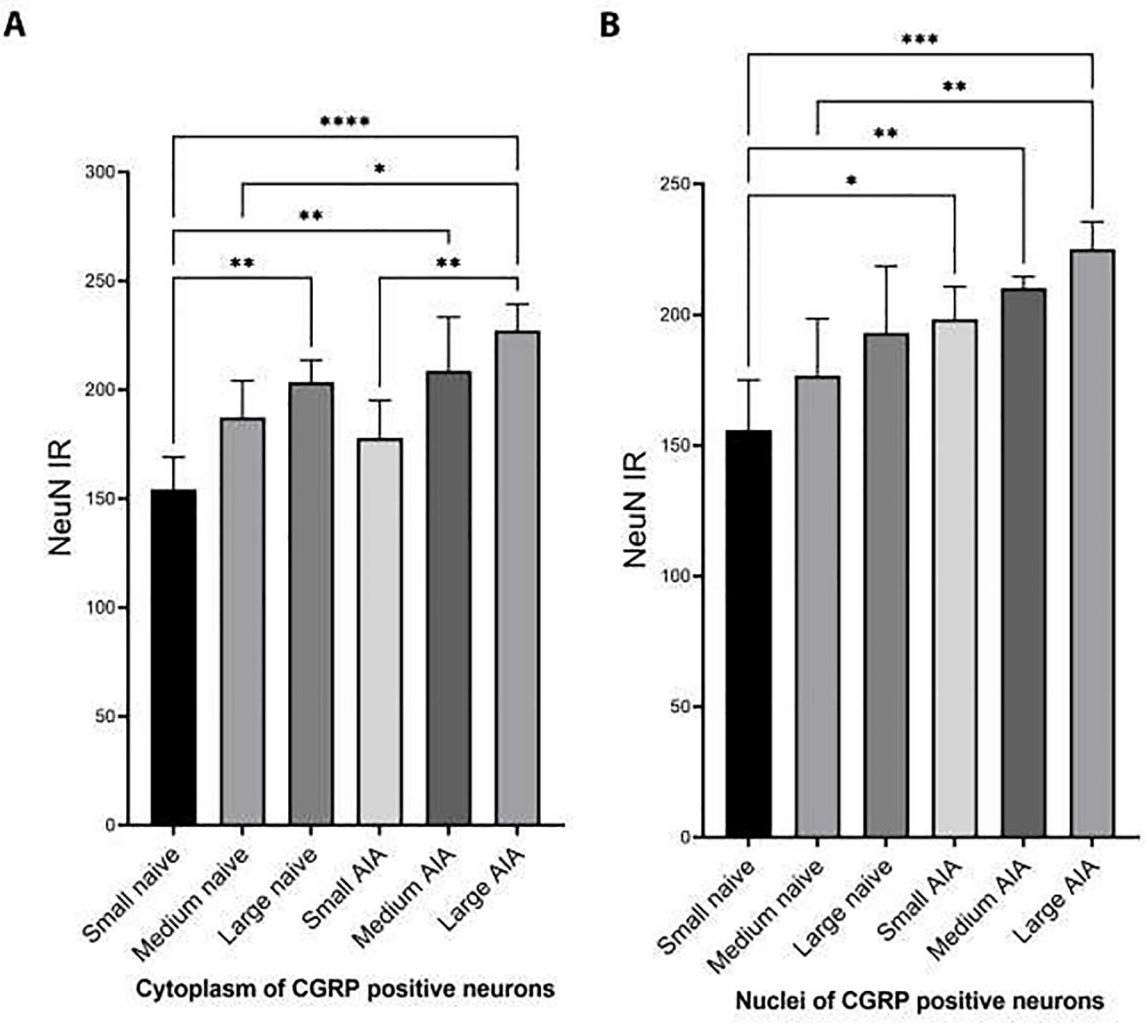

Figure 4: Significant differences of NeuN-IR between size populations for naïve and AIA groups in CGRP (+) and CGRP (−) DRG neurons (D-F).

D, significant differences found in specific size populations and conditions for CGRP (+) cytoplasm ($F(5, 18)=9.530$, $p=0.0001$). **E**, significant differences found in specific size populations and conditions for CGRP (+) nuclei ($F(5,18)=8.087$, $p=0.0004$).

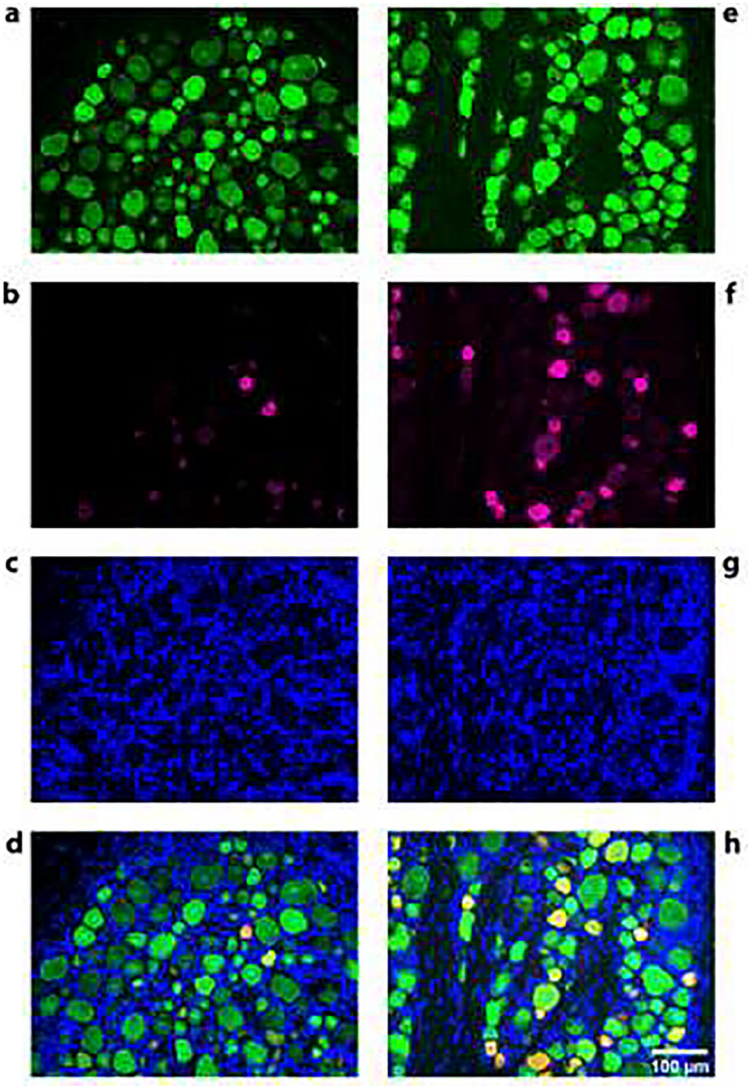

Figure 5: Representative fields-of-view for naïve and inflamed AIA conditions.

A, NeuN, **B**, CGRP, **C,** DAPI, **D**, naïve composite; and AIA group: **E**, NeuN, **F**, CGRP, **G**, DAPI, and **H**, AIA composite.

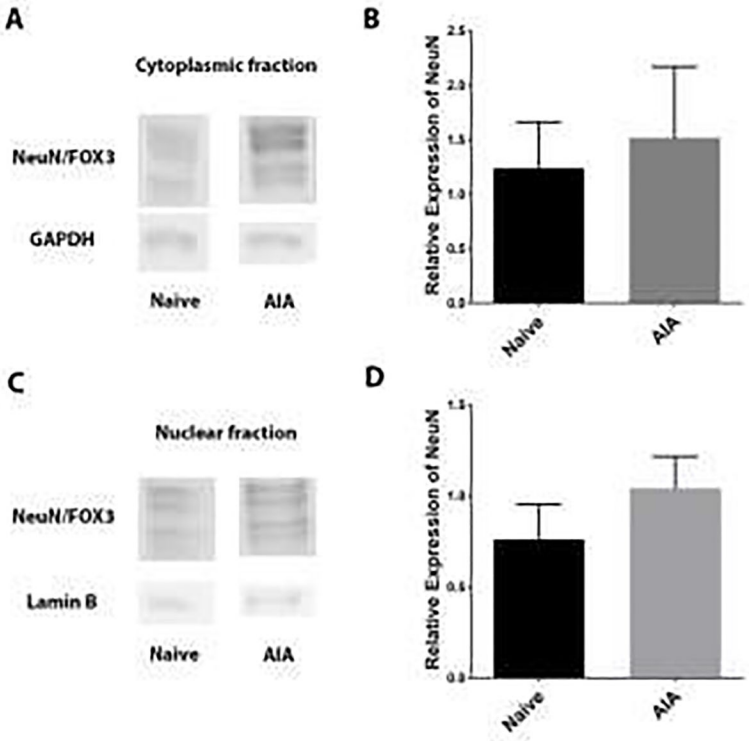

Figure 6: Representative naïve and AIA immunoblot of NeuN.

A, representative NeuN immunoblot from one naïve rat and **B**, graph of NeuN cytoplasmic fractions. **C**, representative NeuN immunoblot from one AIA rat and **D**, graph of NeuN nuclear fractions.

Neurosci Lett. Author manuscript; available in PMC 2022 August 24.

Table 1:

Post-hoc comparisons using Tukey method for NeuN IR between conditions and CGRP (+) and CGRP (−) DRG neuronal cytoplasm and nucleus, for all size populations. in DRG neuronal sub-compartments and size populations.

Location and Size	Test details	Mean 1	Mean 2	Mean Diff.	95.00% CI of diff.	Significant?	Summary	Adjusted P Value	SE of diff.	n1	n2	q	DF
Cytoplasm from **Small** sized neurons	Control cyto (small) cgrp − vs. AIA cyto (small) cgrp −	154.2	169.7	−15.44	−51.09 to 20.21	No	ns	0.588	12.01	4	4	1.818	12
	Control cyto (small) cgrp − vs. Control cyto (small) cgrp +	154.2	154.3	−0.07945	−35.73 to 35.57	No	ns	>.999	12.01	4	4	0.0094	12
	Control cyto (small) cgrp − vs. AIA cyto (small) cgrp +	154.2	177.9	−23.69	−59.34 to 11.96	No	ns	0.251	12.01	4	4	2.79	12
	AIA cyto (small) cgrp − vs. Control cyto (small) cgrp +	169.7	154.3	15.36	−20.29 to 51.01	No	ns	0.592	12.01	4	4	1.809	12
	AIA cyto (small) cgrp − vs. AIA cyto (small) cgrp +	169.7	177.9	−8.25	−43.90 to 27.40	No	ns	0.9	12.01	4	4	0.9716	12
	Control cyto (small) cgrp + vs. AIA cyto (small) cgrp +	154.3	177.9	−23.61	−59.26 to 12.04	No	ns	0.253	12.01	4	4	2.78	12
Cytoplasm from **Medium** sized neurons	Naive CGRP − vs. AIA CGRP −	158.2	178.7	−20.51	−62.28 to 21.26	No	ns	0.49	14.07	4	4	2.062	12
	Naive CGRP − vs. Naive CGRP +	158.2	187.3	−29.12	−70.89 to 12.64	No	ns	0.217	14.07	4	4	2.928	12
	Naive CGRP − vs. AIA CGRP +	158.2	208.8	−50.62	−92.39 to −8.850	Yes	*	0.017	14.07	4	4	5.088	12
	AIA CGRP − vs. Naive CGRP +	178.7	187.3	−8.612	−50.38 to 33.16	No	ns	0.926	14.07	4	4	0.8657	12
	AIA CGRP − vs. AIA CGRP +	178.7	208.8	−30.11	−71.88 to 11.66	No	ns	0.196	14.07	4	4	3.026	12
	Naive CGRP + vs. AIA CGRP +	187.3	208.8	−21.49	−63.26 to 20.27	No	ns	0.452	14.07	4	4	2.161	12
Cytoplasm from **Large** sized neurons	Naive CGRP − vs. AIA CGRP −	140.9	148.8	−7.935	−37.26 to 21.39	No	ns	0.852	9.878	4	4	1.136	12
	Naive CGRP − vs. Naive CGRP +	140.9	203.4	−62.56	−91.88 to −33.23	Yes	***	<.001	9.878	4	4	8.956	12

Location and Size	Test details	Mean 1	Mean 2	Mean Diff.	95.00% CI of diff.	Significant?	Summary	Adjusted P Value	SE of diff.	n1	n2	q	DF
	Naive CGRP − vs. AIA CGRP +	140.9	227.2	−86.34	−115.7 to −57.01	Yes	***	<.001	9.878	4	4	12.36	12
	AIA CGRP − vs. Naive CGRP +	148.8	203.4	−54.62	−83.95 to −25.30	Yes	***	<.001	9.878	4	4	7.82	12
	AIA CGRP − vs. AIA CGRP +	148.8	227.2	−78.4	−107.7 to −49.08	Yes	***	<.001	9.878	4	4	11.22	12
	Naive CGRP + vs. AIA CGRP +	203.4	227.2	−23.78	−53.11 to 5.545	No	ns	0.128	9.878	4	4	3.405	12
Nucleus from **Small**	Control nucleus (small) cgrp − vs. AIA nucleus (small) cgrp −	157.1	186.9	−29.74	−74.48 to 15.00	No	ns	0.251	15.07	4	4	2.791	12
	Control nucleus (small) cgrp − vs. Control nucleus (small) cgrp +	157.1	155.8	1.29	−43.45 to 46.03	No	ns	>.999	15.07	4	4	0.121	12
	Control nucleus (small) cgrp − vs. AIA nucleus (small) cgrp +	157.1	198.4	−41.28	−86.02 to 3.467	No	ns	0.074	15.07	4	4	3.873	12
	AIA nucleus (small) cgrp − vs. Control nucleus (small) cgrp +	186.9	155.8	31.03	−13.72 to 75.77	No	ns	0.221	15.07	4	4	2.912	12
	AIA nucleus (small) cgrp − vs. AIA nucleus (small) cgrp +	186.9	198.4	−11.54	−56.28 to 33.20	No	ns	0.868	15.07	4	4	1.083	12
	Control nucleus (small) cgrp + vs. AIA nucleus (small) cgrp +	155.8	198.4	−42.57	−87.31 to 2.177	No	ns	0.064	15.07	4	4	3.994	12
Nucleus from **Medium** sized neurons	Naive CGRP − vs. AIA CGRP −	164.1	201.1	−36.99	−78.69 to 4.714	No	ns	0.089	14.05	4	4	3.724	12
	Naive CGRP − vs. Naive CGRP +	164.1	176.6	−12.5	−54.20 to 29.20	No	ns	0.81	14.05	4	4	1.258	12
	Naive CGRP − vs. AIA CGRP +	164.1	210.1	−46.02	−87.72 to −4.315	Yes	*	0.029	14.05	4	4	4.633	12
	AIA CGRP − vs. Naive CGRP +	201.1	176.6	24.49	−17.21 to 66.19	No	ns	0.345	14.05	4	4	2.466	12
	AIA CGRP − vs. AIA CGRP +	201.1	210.1	−9.029	−50.73 to 32.67	No	ns	0.916	14.05	4	4	0.9091	12
	Naive CGRP + vs. AIA CGRP +	176.6	210.1	−33.52	−75.22 to 8.180	No	ns	0.133	14.05	4	4	3.375	12

Location and Size	Test details	Mean 1	Mean 2	Mean Diff.	95.00% CI of diff.	Significant?	Summary	Adjusted P Value	SE of diff.	n1	n2	q	DF
Nucleus from **Large** sized neurons	Naive CGRP − vs. AIA CGRP −	147.6	164.8	−17.17	−60.08 to 25.75	No	ns	0.646	14.46	4	4	1.68	12
	Naive CGRP − vs. Naive CGRP +	147.6	193	−45.38	−88.30 to −2.467	Yes	*	0.037	14.46	4	4	4.44	12
	Naive CGRP − vs. AIA CGRP +	147.6	225.1	−77.5	−120.4 to −34.58	Yes	***	<.001	14.46	4	4	7.582	12
	AIA CGRP − vs. Naive CGRP +	164.8	193	−28.22	−71.13 to 14.70	No	ns	0.259	14.46	4	4	2.76	12
	AIA CGRP − vs. AIA CGRP +	164.8	225.1	−60.33	−103.2 to −17.41	Yes	**	0.006	14.46	4	4	5.902	12
	Naive CGRP + vs. AIA CGRP +	193	225.1	−32.11	−75.03 to 10.80	No	ns	0.173	14.46	4	4	3.142	12

Neurosci Lett. Author manuscript; available in PMC 2022 August 24.

Table 2:

Post-hoc comparisons using Tukey method for evaluating size populations within naïve and AIA conditions for CGRP (+) and CGRP (−) DRG neurons.

Condition and Class	Test details	Mean 1	Mean 2	Mean Diff.	95.00% CI of diff.	Significant?	Summary	Adjusted P Value	SE of diff.	n1	n2	q	DF
Naïve Cytoplasm (CGRP negative)	Small vs. Medium	154.2	158.2	−3.969	−29.86 to 21.92	No	ns	0.905	9.273	4	4	0.605	9
	Small vs. Large	154.2	140.9	13.36	−12.53 to 39.25	No	ns	0.362	9.273	4	4	2.038	9
	Medium vs. Large	158.2	140.9	17.33	−8.561 to 43.22	No	ns	0.2029	9.273	4	4	2.643	9
Naïve Cytoplasm (CGRP positive)	Small vs. Medium	154.3	187.3	−33.01	−61.06 to −4.970	Yes	*	0.0232	10.04	4	4	4.648	9
	Small vs. Large	154.3	203.4	−49.12	−77.16 to −21.07	Yes	**	0.0022	10.04	4	4	6.916	9
	Medium vs. Large	187.3	203.4	−16.1	−44.15 to 11.94	No	ns	0.2933	10.04	4	4	2.267	9
Naïve Nucleus (CGRP negative)	Small vs. Medium	157.1	164.1	−7.018	−50.88 to 36.85	No	ns	0.897	15.71	4	4	0.632	9
	Small vs. Large	157.1	147.6	9.501	−34.36 to 53.37	No	ns	0.8211	15.71	4	4	0.855	9
	Medium vs. Large	164.1	147.6	16.52	−27.35 to 60.38	No	ns	0.5653	15.71	4	4	1.487	9
Naïve Nucleus (CGRP positive)	Small vs. Medium	155.8	176.6	−20.8	−64.98 to 23.38	No	ns	0.4225	15.82	4	4	1.859	9
	Small vs. Large	155.8	193	−37.17	−81.35 to 7.009	No	ns	0.0993	15.82	4	4	3.322	9
	Medium vs. Large	176.6	193	−16.37	−60.55 to 27.81	No	ns	0.5752	15.82	4	4	1.463	9
AIA Cytoplasm (CGRP negative)	Small vs. Medium	169.7	178.7	−9.043	−50.87 to 32.79	No	ns	0.8218	14.98	4	4	0.854	9
	Small vs. L arge	169.7	148.8	20.87	−20.97 to 62.70	No	ns	0.3844	14.98	4	4	1.97	9
	Medium vs. Large	178.7	148.8	29.91	−11.92 to 71.74	No	ns	0.1687	14.98	4	4	2.823	9
AIA Cytoplasm (CGRP positive)	Small vs. Medium	177.9	208.8	−30.9	−67.83 to 6.025	No	ns	0.1013	13.23	4	4	3.304	9
	Small vs. Large	177.9	227.2	−49.29	−86.21 to −12.36	Yes	*	0.0118	13.23	4	4	5.271	9
	Medium vs. Large	208.8	227.2	−18.39	−55.31 to 18.54	No	ns	0.3855	13.23	4	4	1.966	9
AIA Nucleus (CGRP negative)	Small vs. Medium	186.9	201.1	−14.27	−62.66 to 34.13	No	ns	0.6989	17.33	4	4	1.164	9
	Small vs. Large	186.9	164.8	22.07	−26.33 to 70.47	No	ns	0.4436	17.33	4	4	1.801	9
	Medium vs. Large	201.1	164.8	36.34	−12.06 to 84.73	No	ns	0.1455	17.33	4	4	2.965	9
AIA Nucleus (CGRP positive)	Small vs. Medium	198.4	210.1	−11.76	−30.85 to 7.336	No	ns	0.2505	6.839	4	4	2.431	9
	Small vs. Large	198.4	225.1	−26.72	−45.81 to −7.625	Yes	**	0.009	6.839	4	4	5.525	9
	Medium vs. Large	210.1	225.1	−14.96	−34.06 to 4.134	No	ns	0.127	6.839	4	4	3.094	9